



CORPORATE PARTNER

WHITE PAPER

Nanoscale impedance and permittivity properties at microwave frequencies using SMM

Ferry Kienberger, Keysight Technologies Austria GmbH

Georg Gramse, Johannes Kepler University, Biophysics Institute

Scanning microwave microscopy (SMM) is a nanoscale characterization technique used to extract accurate materials properties, including electrical, magnetic, and dielectric properties, at microwave frequencies (1–20 GHz). In comparison to scanning capacitance microscopy, the SMM works at higher broadband frequencies measuring absolute impedance values, including calibrated capacitance and conductance of the sample. For a given capacitance value, the higher the measurement frequency, the higher the complex impedance signal. Accordingly, sensitive measurements can be completed with SMM, and small impedances can be measured, which is useful to study small semiconductor devices, thin materials layers (e.g., 2D materials), and tiny biological cell compartments (e.g., membranes and viruses). SMM interfaces two well-known measurement tools: the atomic force microscope (AFM) for nanoscale imaging and the vector network analyzer (VNA) for high-frequency signal measurements and materials analyses.¹ The AFM allows for nanometer lateral resolution imaging, and the VNA provides high precision impedance and admittance measurements.

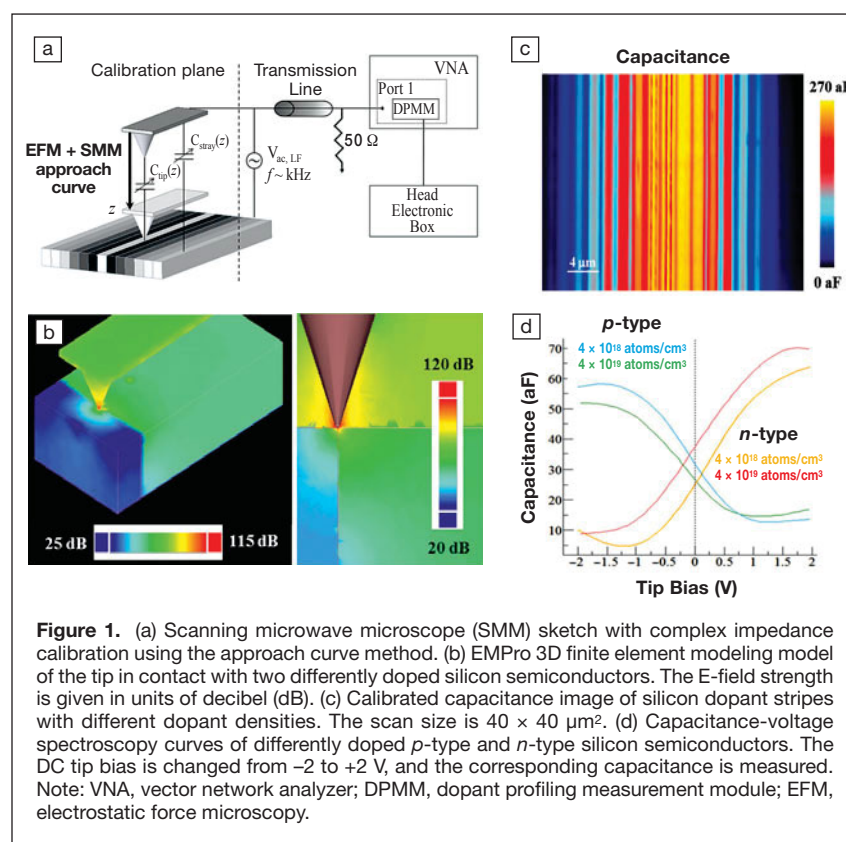
The conductive tip acts both as a nanometer scale AFM probe and as a GHz emitter-receiver antenna. The VNA reflection scattering signal is measured and converted to meaningful physical quantities, such as complex impedance and admittance, by means of a SMM calibration procedure. This article reviews the calibration and application

of SMM to determine various electric, magnetic, and dielectric materials properties, including resistivity, conductance, dielectric constant, complex permittivity, and magnetic permeability.

The SMM merges the nanoscale imaging capabilities of AFM with the high-frequency broadband impedance measurement accuracy of VNA (Figure 1a). SMM allows for nanoscale impedance imaging and doping profiling of semiconductor materials using a microwave signal. Typically the SMM is operated in reflection mode, whereby the ratio of the reflected and incident

electromagnetic waves, the so-called scattering parameter S_{11} , is measured by the VNA at each pixel of the AFM tip-sample contact point. A microwave image is generated pixel by pixel simultaneously with the topographical imaging of the sample.

There are two main imaging modes in SMM. The first is quantitative dopant profiling by means of differential capacitance (also called dC/dV), which is a widely used technique for semiconductor failure analysis and detecting leakages in solid-state devices with nanometer resolution.² The dC/dV mode relies on a low-frequency (kHz) modulation of the GHz



Keysight Technologies

The MRS Corporate Partner Program supports the Materials Research Society Foundation.



signal that allows tuning the semiconductor depletion zone and probing the doping concentration. The second SMM mode is complex impedance imaging, and it is based directly on the scattering S_{11} signal. The S_{11} signal is detected by VNA and depends on the tip-sample relative electrical impedance. A calibration workflow was developed that allows converting the raw S_{11} into calibrated capacitance and resistance images using approach curves (Figure 1a–b).^{3,4} The calibrated capacitance images typically range from 100 aF (attofarad) to 1 fF (femtofarad) at 20 GHz, as shown in Figure 1c, for a silicon semiconductor sample with various doping concentrations.⁵ The corresponding SMM resistance and conductance images typically show 0.1–100 M Ω (mega-ohms) and 0.01–10 μ S (microsiemens), respectively.

From the calibrated complex impedance images (i.e., capacitance and resistance), material properties can be determined quantitatively. First, the capacitance can be converted to the dielectric constant using appropriate tip-sample geometrical models ranging from analytical formulas of thin films to complex 3D finite element modeling (FEM) of irregularly shaped structures.³ The method was verified for various oxides ranging from SiO₂ with $\epsilon = 4$ to high- k oxides such as SrTiO₃ with $\epsilon = 300$.⁶ Second, the resistance and conductance can be converted to resistivity and conductivity, respectively, using a tip-sample analytical model that includes tip radius, microwave penetration skin depth, and semiconductor depletion layer width.⁵

The method has been tested on doped silicon samples, and the resistivity and doping concentration are in quantitative agreement with data sheet values over a range of 10⁻³ Ω *cm to 10¹ Ω *cm, and 10¹⁴ atoms/cm³ to 10²⁰ atoms/cm³, respectively. The lateral resolution of SMM is limited by the AFM tip probe apex radius to roughly 10 nm, while the bulk penetration is mainly determined by the skin depth. The skin depth and therefore the microwave penetration depth can be changed by varying the SMM frequency. In this way, frequency-dependent depth profiling can be realized with SMM.⁵

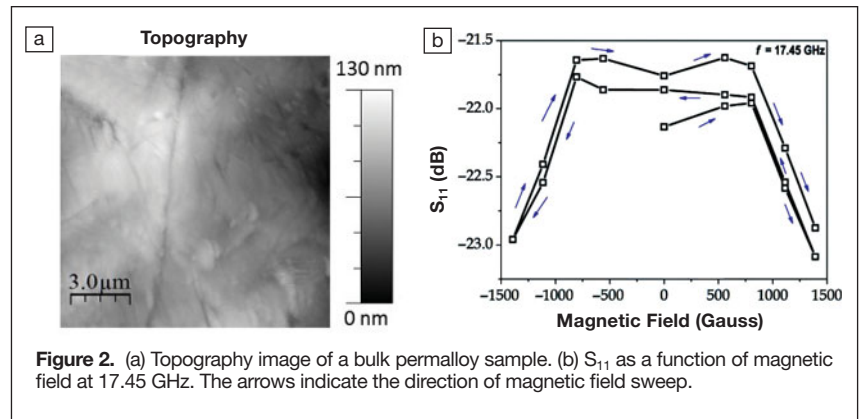


Figure 2. (a) Topography image of a bulk permalloy sample. (b) S_{11} as a function of magnetic field at 17.45 GHz. The arrows indicate the direction of magnetic field sweep.

Figure 1d shows capacitance-voltage (C-V) spectroscopy curves for material physics investigations. The nanoscale lateral resolution of SMM allows imaging of doped regions, interfaces, and junctions at different tip DC-voltage bias. The capacitance depends on the doping density and reaches 300 aF, with high capacitance values observed on highly doped silicon regions.⁷

The Keysight 3D FEM software EMPro can model the GHz electric and magnetic field distribution of the nanoscale tip-sample region. Figure 1b shows nanoscale modeling of the E-field and impedance values of the SMM tip-sample system at 20 GHz.^{7,8}

Figure 2 shows microwave frequency characterization of magnetic materials for analyzing and imaging local magnetic properties at the nanoscale.⁹ The changes of the magnetic properties of yttrium iron garnet films and permalloy samples have been studied as a function of external DC magnetic bias (Figure 2a, b). Bulk permalloy samples were imaged with different external field strengths, including 225 and 330 Oe (Oersteds), showing that the magnetic properties of the two regions change with the external field. A hysteretic behavior of the reflection coefficient S_{11} was observed with an external bias field applied perpendicular to the sample surface. Further experiments were completed to prove that changes in the impedance of the tip-sample system come only from the changes in the magnetic properties (i.e., from the inductive part of the impedance) and not from any capacitive changes. The magnetic bias does not alter the capacitive

part, which is related to the dielectric constant of the material and not to the magnetic permeability.⁹

SMM can be used for various materials science applications, including nanoscale electrical, dielectric, and magnetic measurements. Advanced calibration workflows are available for complex impedance imaging and dielectric quantification. Voltage and impedance spectroscopy studies can be applied to nanoscale semiconductor devices, advanced materials, and bio-samples in water solutions at broadband microwave frequency.

References

1. H.P. Huber, M. Moetelmaier, T.M. Wallis, C.J. Chiang, M. Hochleitner, A. Imtiaz, Y.J. Oh, K. Schilcher, M. Dieudonne, J. Smoliner, P. Hinterdorfer, S.J. Rosner, H. Tanbakuchi, P. Kabos, F. Kienberger, *Rev. Sci. Instrum.* **81**, 113701 (2010).
2. H.P. Huber, I. Humer, M. Hochleitner, M. Fenner, M. Moetelmaier, *J. Appl. Phys.* **111**, 014301 (2012).
3. G. Gramse, M. Kasper, L. Fumagalli, G. Gomila, P. Hinterdorfer, F. Kienberger, *Nanotechnology* **25**, 145703 (2014).
4. M. Kasper, G. Gramse, F.F. Kienberger, *Proc. IEEE Int. Microwave Symp.* (May 2016), pp. 1–4, doi:10.1109/MWSYM.2016.7540183.
5. E. Brinciotti, G. Gramse, S. Hommel, T. Schweinboeck, A. Altes, M.A. Fenner, J. Smoliner, M. Kasper, G. Badino, S.-S. Tuca, F. Kienberger, *Nanoscale* **7**, 14715 (2015).
6. J. Hoffmann, G. Gramse, J. Niegemann, M. Zeier, F. Kienberger, *Appl. Phys. Lett.* **105**, 013102 (2014).
7. E. Brinciotti, G. Campagnaro, G. Badino, M. Kasper, G. Gramse, S.S. Tuca, J. Smoliner, T. Schweinboeck, S. Hommel, F. Kienberger, *IEEE Trans. Nanotechnol.* **16**, 75 (2017).
8. A.O. Oladipo, M. Kasper, S. Lavdas, G. Gramse, F. Kienberger, N.C. Panou, *Appl. Phys. Lett.* **103**, 213106 (2013).
9. C.H. Joseph, G.M. Sardi, S.S. Tuca, G. Gramse, A. Lucibello, E. Proietti, F. Kienberger, R. Marcelli, *J. Magn. Magn. Mat.* **420**, 62 (2016). □